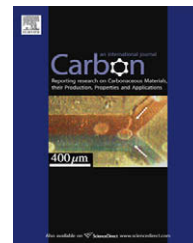


available at www.sciencedirect.comjournal homepage: www.elsevier.com/locate/carbon

Effect of activation time on the properties of activated carbons prepared by microwave-assisted activation for electric double layer capacitors

Xiaojun He ^{a,*}, Yejing Geng ^a, Jieshan Qiu ^{b,*}, Mingdong Zheng ^a, Suan Long ^a, Xiaoyong Zhang ^a

^a School of Chemistry and Chemical Engineering, Anhui Key Lab of Coal Clean Conversion and Utilization, Anhui University of Technology, Ma'anshan 243002, China

^b Carbon Research Laboratory, State Key Lab of Fine Chemicals, School of Chemical Engineering, Dalian University of Technology, 158 Zhongshan Road, P.O. Box 49, Dalian 116012, China

ARTICLE INFO

Article history:

Received 17 November 2009

Accepted 12 January 2010

Available online 15 January 2010

ABSTRACT

Activated carbons (ACs) were prepared by microwave-assisted heat treatment of petroleum coke with KOH as activation agent, and characterized by infrared spectroscopy and nitrogen adsorption technique with the aim of studying the effect of activation time on the properties of ACs for electrodes in electric double layer capacitors (EDLCs). The electrochemical properties of AC electrodes in EDLCs were studied by cyclic voltammetry, constant current charge–discharge and electrochemical impedance spectroscopy. The results show that the specific surface area (S_{BET}) and total pore volume of ACs goes through a maximum as the activation time increases. At 35 min of the activation time, the as-made AC (denoted as AC-35) has a S_{BET} of 2312 m²/g. With AC-35 as the electrode, its specific capacitance in EDLC at a current density of 50 mA/g can reach 342.8 F/g, and remains at 245.6 F/g even after 800 cycles while the energy density of the capacitor remains at 8.0 Wh/kg. The results have demonstrated that the microwave-assisted heat treatment is an efficient approach to the preparation of ACs with high performance for EDLCs.

© 2010 Elsevier Ltd. All rights reserved.

1. Introduction

The electric double layer capacitor (EDLC) is a new energy storage device with high power density and long lifetime that is better than traditional batteries [1], and has been used in many fields such as mobile communication and electric vehicles. EDLCs are based on electrochemical charge accommodation at the electric double layer and the occurrence of Faradic reactions [2–6], of which the performance depends on the electrode materials to a great degree. Activated carbons (ACs) have been widely used as the EDLC electrode materials because of its unique physicochemical properties, good con-

ductivity and low cost [3], which can be prepared from different carbon sources by heat treatment and activation [7–11]. To date, microwave-assisted heat treatment method has drawn much attention because of its fast and uniform heating capability, which makes it possible to make ACs with high surface area and well-developed porous structure, at the same time, to consume less energy compared with the conventional heat treatment methods. For ACs, their specific capacitance is usually proportional to their specific surface area. The ideal ACs for EDLC electrodes are required to have a high surface area and an optimal pore size distribution that are important to high specific capacitance of EDLCs [12]. Here we report on

* Corresponding authors. Fax: +86 555 2311822 (X. He), fax: +86 411 39893991 (J. Qiu).

E-mail addresses: xjhe@ahut.edu.cn (X. He), jqiu@dlut.edu.cn (J. Qiu).
0008-6223/\$ - see front matter © 2010 Elsevier Ltd. All rights reserved.
doi:10.1016/j.carbon.2010.01.016

microwave-assisted KOH activation of petroleum coke for preparing ACs with high performance for EDLCs. The effect of activation time on AC properties has been systematically studied in terms of the EDLC performance.

2. Experimental

2.1. Preparation and characterization of ACs

Petroleum coke (<74 μm in particle size) from Daqing oil field of China was used as raw material to prepare ACs, of which the proximate analysis and elemental analysis data are shown in Table 1. M_{ad} is the water content in petroleum coke on the air dry basis, A_{d} is the ash content in petroleum coke on the dry basis, and V_{daf} is the content of volatile matter in petroleum coke on dry and ash free basis.

For each run, the petroleum coke was first mixed with KOH in a weight ratio of 1:5. The mixture was dried under vacuum at 80 $^{\circ}\text{C}$ for 2 h to remove water, and then put in a corundum crucible with a lid in which there was a small gas hole. The crucible was surrounded by a cylindric Al_2O_3 fiber composite, and heated in a LWMC-205-type microwave oven with an output power of 250 W. The temperature of the sample in the crucible was monitored by a thermal couple. The as-made ACs were washed with deionized water till the pH of the washing solution reached ca. 7, then dried at 120 $^{\circ}\text{C}$ for 2 h under vacuum before use.

The as-made ACs were characterized by Fourier transform infrared spectrometry (FT-IR), and N_2 adsorption technique. Before the liquid N_2 adsorption at 77 K, the ACs were degassed at 250 $^{\circ}\text{C}$ in flowing N_2 for 4 h under vacuum. For the as-made ACs, the specific surface area was calculated using the BET equation, the pore size distribution was determined by BJH method, and the micropore size distribution was determined by micropore analysis method and t-plot method, while the total pore volume was assumed to be the liquid volume of adsorbed N_2 at a relative pressure of 0.99.

2.2. Preparation of AC electrode

The EDLC electrodes were made of ACs, carbon black (CB) and poly(tetrafluoroethylene) (PTFE), in which AC was the base material, and CB with a specific surface area of 550 m^2/g (Cabot-Corp., China) functioned as a conducting material. For a typical run, the AC, CB and PTFE were mixed in a weight ratio of 89:5:6, the mixture was pressed onto a foam nickel with a size of 1.5 \times 1.5 cm (the nickel foam functions as the current collector), yielding electrodes with a height of ca. 0.6 mm and with an active mass of ca. 120 mg. Before the EDLC test, the electrodes were dried at 120 $^{\circ}\text{C}$ for 2 h under vacuum.

2.3. Electrochemical measurements of AC electrodes

The as-made AC electrodes were tested using cyclic voltammetry and electrochemical impedance spectroscopy (EIS) in an electrochemical workstation (CHI-760C, China). The test cell was made of two electrodes, and tested in 6 M KOH and LiOH mixture solution at a KOH/LiOH weight ratio of 50:1 with a symmetrical cell configuration. Before the test, the cell was soaked in the KOH/LiOH mixture solution for 1 h under vacuum. The capacitance behavior of AC electrodes was examined at a constant current discharge mode (LAND, CT-2001A). The tests of the electrodes include stabilization at a current density of 50 mA/g for 15 cycles under constant current charge–discharge conditions, discharge at different current density (20, 50, 100, 200 and 300 mA/g), and charge–discharge at different current density (50, 100 and 200 mA/g) as well as multi-cycle charge–discharge at a current density of 50 mA/g.

3. Results and discussion

3.1. FT-IR analysis

Fig. 1 is the FT-IR spectra of ACs made in different activation time, showing that there is not much difference in the surface properties of the as-made ACs. The peak at 3440 cm^{-1} is due to the –O–H stretching vibration, and the band at 2925 cm^{-1} is due to the –C–H stretching. The peak at 1633 cm^{-1} is the characteristic of –C=O stretching vibration of carbonyl groups [13,14]. The peak at 1384 cm^{-1} is due to the –C–H stretching vibration [15]. The band at 1117 cm^{-1} is due to the –C–O stretching vibration. The weak peaks at 620 and 2297 cm^{-1} are difficult to assign though they are mentioned in the literature [16]. It should be noted that the peak intensity of –C=O at 1633 cm^{-1} or –C–O at 1117 cm^{-1} for AC-31 sample is higher than other samples, implying that the intensity of oxygen-containing functional groups in the as-made ACs can be tuned to some degree by changing the activation time.

3.2. Pore structure characterization

The N_2 adsorption–desorption isotherms of ACs made in different activation time are shown in Fig. 2, showing that all of the as-made ACs are microporous materials, evidenced by the Type I isotherms. No obvious hysteresis loop can be seen in the adsorption–desorption isotherms for all of the as-made AC samples. When the relative pressure (P/P_0) is below 0.1, N_2 adsorption increases quickly for all of the as-made ACs. In the case of AC-35 sample, this trend continues till the relative pressure reaches 0.2. The adsorption at lower pres-

Table 1 – The proximate analysis and elemental analysis of petroleum coke.

Sample	Proximate analysis (wt.%)			Elemental analysis (daf, wt.%)				
	M_{ad}	A_{d}	V_{daf}	C	H	S	N	O ^a
Petroleum coke	1.20	0.21	12.49	90.30	4.26	0.81	1.79	2.84

^a By difference.

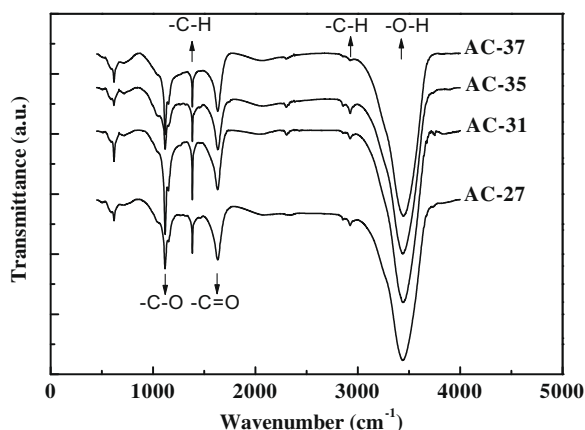


Fig. 1 – FT-IR spectra of ACs made by microwave-assisted activation in different activation time.

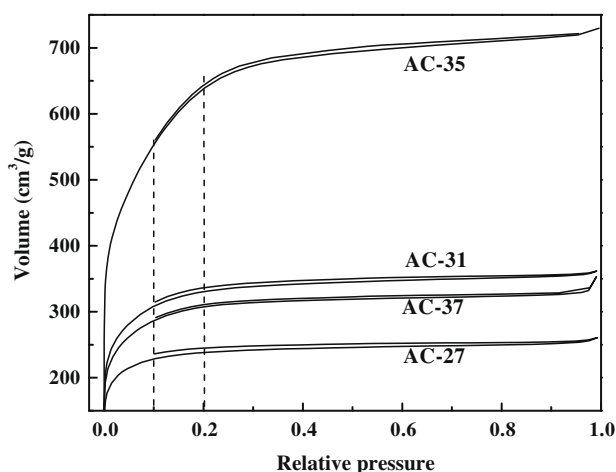


Fig. 2 – N₂ adsorption–desorption isotherms of ACs made by microwave-assisted activation in different time.

sure is indicative of micropore structure. The pore structure parameters of ACs are summarized in Table 2.

Table 2 shows that for the as-made ACs, the S_{BET} , V_t , V_{mic} and $V_{\text{mes+mac}}$ goes through a maximum as the activation time increases from 27 to 37 min, respectively. For AC-35, its S_{BET} is 2312 m²/g and its V_t is 1.13 cm³/g, which is the highest among the four AC samples. For all of the as-made ACs, their V_{mic}/V_t ratio is in a range of 90.7–94.6%, further evidencing that the as-made ACs are microporous. This demonstrates that microwave-assisted heat activation can lead to ACs with high surface area and large pore volume. This is also evidenced by

other reports about the microwave-assisted preparation of ACs from different types of carbon sources [9,11].

Fig. 3 shows the variation of the activation temperature with the microwave heating time. It can be seen from Fig. 3 that the activation temperature reaches 800 °C in 30 min, and then levels off at 800 °C due to the limited output power of the microwave oven used for the heat treatment. During the activation step, the average heating rate is ca. 26.7 °C/min. The quick rise in the temperature due to the microwave heating makes it possible for the coke to be quickly yet efficiently activated by reaction with KOH [17]. The chemical reactions between carbons and KOH have been explained in the literature [18]. Zhang et al. [19] once reported on the production of oxygen-rich ACs from coal by KOH activation at 700 °C with a heating rate of 20 °C/min, yielding an AC with S_{BET} of 1950 m²/g and V_t of 1.10 cm³/g.

The effect of activation time on the pore volume of ACs is shown in Fig. 4, showing that as the activation time increases, the AC pore volume goes through a maximum at 35 min. For the AC-35 sample, its micropore size varies in a range of 0.7–1.1 nm.

3.3. Electrochemical characterizations

3.3.1. Cyclic voltammetry behavior of AC electrodes

Fig. 5 is the cyclic voltammetry curves of AC electrodes obtained at a scan rate of 2 mV/s in 6 M KOH and LiOH aqueous solution, showing that all sweep curves are symmetric on the positive and negative sweeps, and the current at 0 V for electrodes made of different ACs are different from each other. The electrode made of AC-35 is the best among the four ACs tested, evidenced by the high current and the almost ideal standard rectangle. This is in good agreement with the large S_{BET} , V_{mic} and V_t of the AC-35 sample discussed above. With the increase of the activation time from 27 to 35 min, the cyclic voltammetry shape of AC electrodes becomes ideal square cyclic voltammograms, indicating that the electric conductivity properties of AC are greatly improved. However, the current of AC-37 electrodes decreases after the activation time further increase to 37 min, as shown in Fig. 5, implying that the electric conductivity properties of AC-37 electrode become poor. Obviously, the electric conductivity of AC-35 is the best among the four AC electrodes tested. This phenomenon will be further discussed in Section 3.3.2. Rectangular cyclic voltammetry shape of AC-35 electrodes implies a quick dynamics and good charge propagation of AC-35 sample.

3.3.2. Charge–discharge behavior of AC electrodes

Constant current charge–discharge is conducted to measure the specific capacitance of AC electrodes. Fig. 6 is the lin-

Table 2 – Pore structure parameters of ACs.

Sample	S_{BET} (m ² /g)	V_t (cm ³ /g)	V_{mic} (cm ³ /g)	$V_{\text{mes+mac}}$ (cm ³ /g)	V_{mic}/V_t (%)	$V_{\text{mes+mac}}/V_t$ (%)
AC-27	792	0.40	0.37	0.03	93.5	7.5
AC-31	1121	0.56	0.53	0.03	94.6	5.4
AC-35	2312	1.13	1.05	0.08	92.9	7.1
AC-37	1053	0.54	0.49	0.05	90.7	9.3

S_{BET} , BET surface area; V_{mic} , volume of micropore (<2 nm); $V_{\text{mes+mac}}$, volume of mesopore and macropore; V_t , total pore volume.

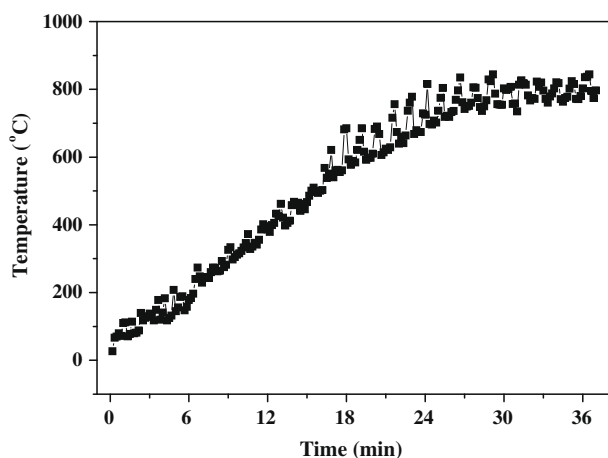


Fig. 3 – The temperature variation of the sample with the microwave heating time.

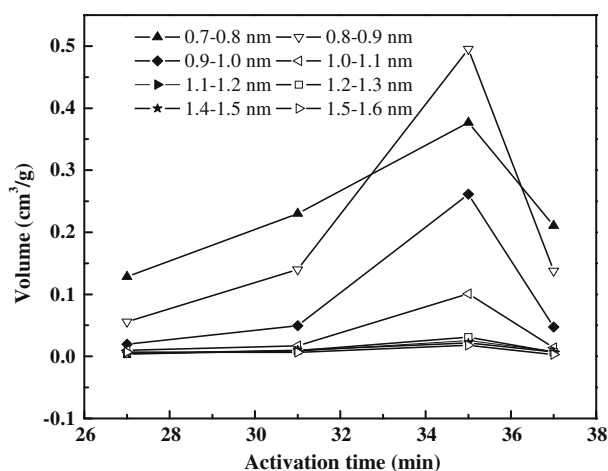


Fig. 4 – Effect of activation time on the pore volume of ACs with different pore size.

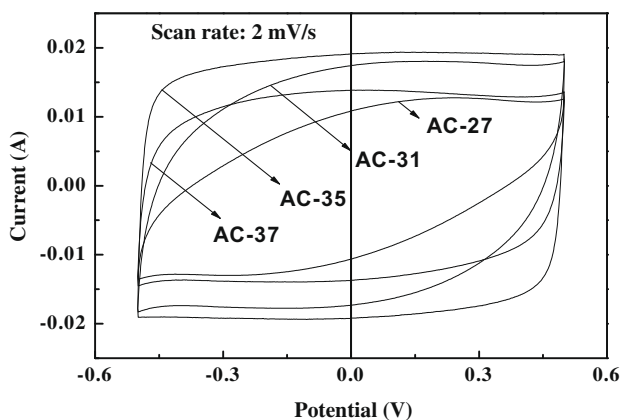


Fig. 5 – Cyclic voltammetry curves of different AC electrodes.

ear voltage–time dependence of AC-35 and AC-37 electrodes, showing that the AC electrodes have the typical capacitive behavior and good charge–discharge reversibility, which is consistent with the cyclic voltammetry behavior of AC elec-

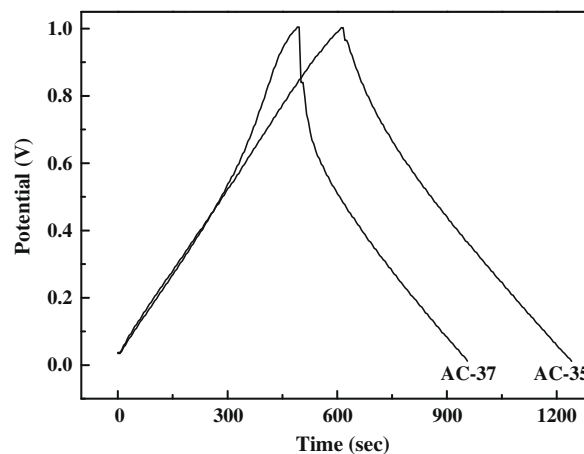


Fig. 6 – Charge–discharge curves of AC electrodes at a current density of 100 mA/g.

trodes shown in Fig. 5. The specific capacitance of the electrode in EDLC can be calculated from the slope of the discharge curve [20,21]. The specific capacitance of AC electrodes measured at a current density of 100 mA/g after 17 times of discharge goes through a maximum with the increase of activation time, which is 125.4 F/g for AC-27, 251.6 F/g for AC-31, 287.8 F/g for AC-35 and 270.3 F/g for AC-37, respectively. It is known that for the EDLCs, their specific capacitance is governed by the accessibility of aqueous solutions to the micropores in ACs. In other words, the micropores in ACs that N_2 molecules can enter at 77 K would function as space for the electro-adsorption of hydrated ions in EDLCs [22,23]. In principle, the pores larger than 0.5 nm are electrochemically accessible for aqueous solutions. In our case, the high capacitance of AC-35 electrode (e.g. 287.8 F/g for AC-35) in KOH and LiOH solutions is in proportion to its large V_t (1.13 cm³/g) and S_{BET} (2312 m²/g) measured by the N_2 adsorption. In general, specific capacitance of AC electrode increases with surface area [24].

The equivalent series resistance (ESR) of AC electrode at the discharge beginning can be calculated according to the discharge curve [25]. The ESR of AC electrodes measured at a current density of 100 mA/g after 17 times of discharge goes through a minimum with the increase of activation time, which is 24.4 Ω for AC-27, 19.4 Ω for AC-31, 1.2 Ω for AC-35 and 6.8 Ω for AC-37, respectively. In other words, the electric conductivity properties of AC electrode go through a maximum with the increase of activation time. These results are in good agreement with the rectangular cyclic voltammetry shape of AC-35 electrodes in Fig. 5. The effect of cycle number on the specific capacitance and ESR of AC-35 electrode at a current density of 50 mA/g is shown in Fig. 7(a) and (b). Fig. 7(a) shows that the specific capacitance of AC-35 electrode decreases from 342.8 to 273.9 F/g after 100 cycles, and then levels off at about 245.6 F/g with a capacitance retention ratio of 71.6% after 800 cycles. The high specific capacitance of AC-35 in KOH and LiOH solutions is also partly due to the presence of LiOH in the KOH electrolyte. Varma and Rempe [26] reported that the Li^+ and K^+ ions would strongly coordinate with water molecules in aqueous solutions. For K^+ ions, the hydration number is 6, and for Li^+ , the hydration number

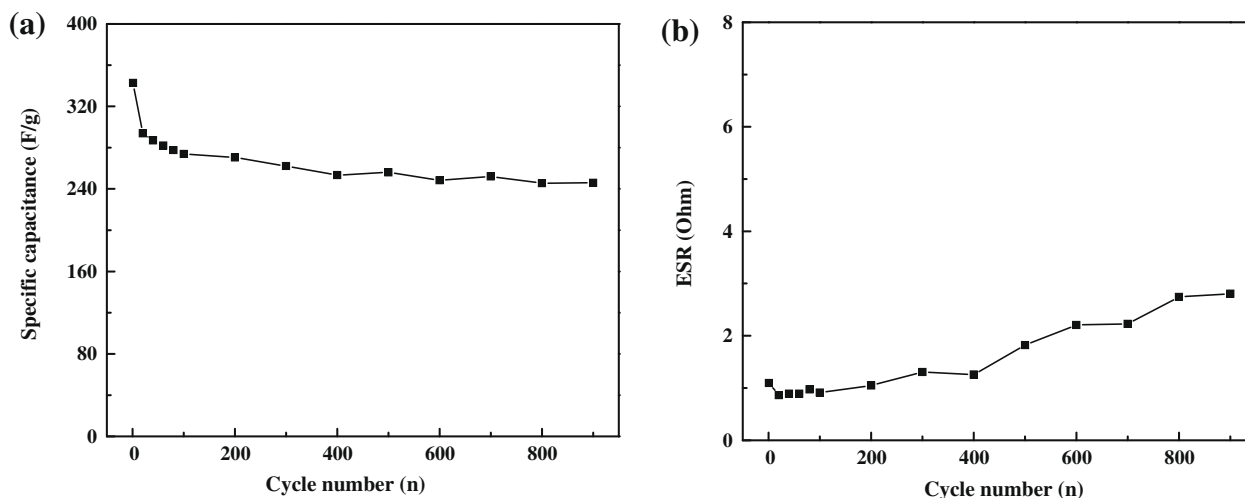


Fig. 7 – Effect of cycle number on specific capacitance of AC-35 electrode (a) and ESR of AC-35 electrode (b).

is 4; this is because the radius of K^+ ion is bigger than that of Li^+ ion in aqueous solutions. The Li^+ ions with smaller hydration number in LiOH electrolyte can move faster, and can reach smaller pores in AC electrode than the K^+ ions. This is one of the reasons why better electrochemical performance is observed in LiOH and KOH mixture electrolyte.

Fig. 7(b) shows that the ESR of AC-35 electrode does not change much as the cycle number increases. Before 100 cycles, the ESR of AC-35 electrode is ca. 1.0Ω , and then increases slowly and reaches 2.7Ω after 800 cycles. This implies that after repeated uses, the capacitors with AC as electrodes will inevitably lose some capacitance, at the same time, the resistance will increase to some degree [27].

For EDLCs made of AC-35 and AC-37, the energy density is plotted against the power density of the capacitors, as shown in Fig. 8(a). The energy density of capacitors is calculated according to Eq. (1) [28].

$$E = \frac{1}{2} CV^2 \quad (1)$$

where C is the capacitance of the two-electrode capacitor (F), V is the voltage decrease or the usable voltage (V) excluding the IR drop occurring at the discharge beginning [23,29].

The power density is calculated according to Eq. (2).

$$P = \frac{VI}{m} \quad (2)$$

where I is the discharge current (mA) and m is the active mass in the two-electrode capacitor (g).

It can be seen from Fig. 8(a) that the energy density of AC-35 capacitor is consistently higher than the AC-37 capacitor, and as the power density increases, the drop of energy density for AC-35 capacitor is smaller than the AC-37 capacitor. For the AC-35 capacitor, the retention ratio of energy density is as high as 83.9% while in the case of AC-37 capacitor, it is only 54.7%. The energy density of AC-35 capacitor remains high at higher power density. This can be ascribed to the large micropore volume ($1.05 \text{ cm}^3/\text{g}$, AC-35) for energy storage [30], and the presence of some mesopore and macropore volume ($0.08 \text{ cm}^3/\text{g}$, AC-35) for ion transport, i.e. mesopores and

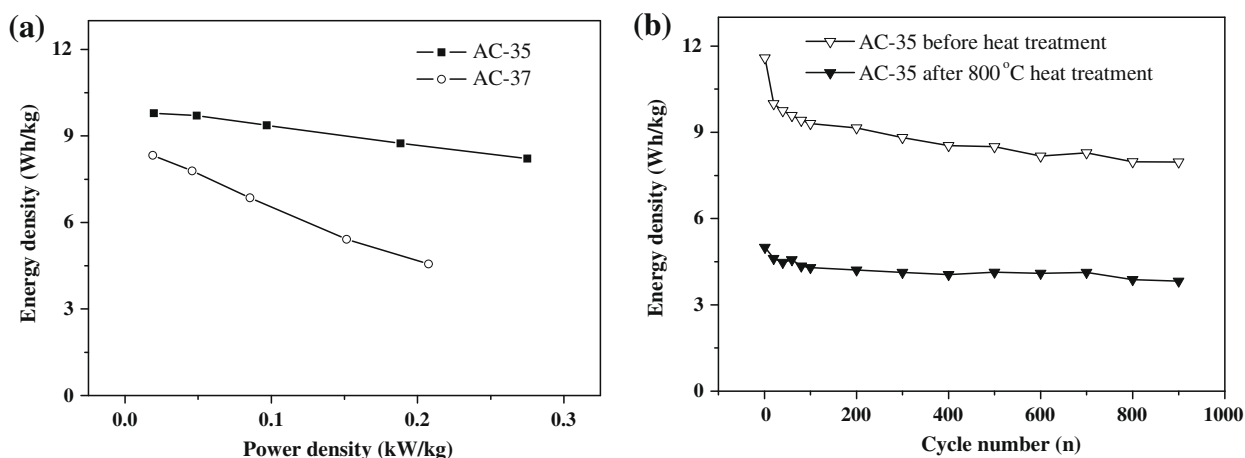


Fig. 8 – (a) Energy density vs. power density of capacitors made of AC-35 and AC-37, (b) energy density vs. cycle number of capacitors made of AC-35 before and after heat treatment.

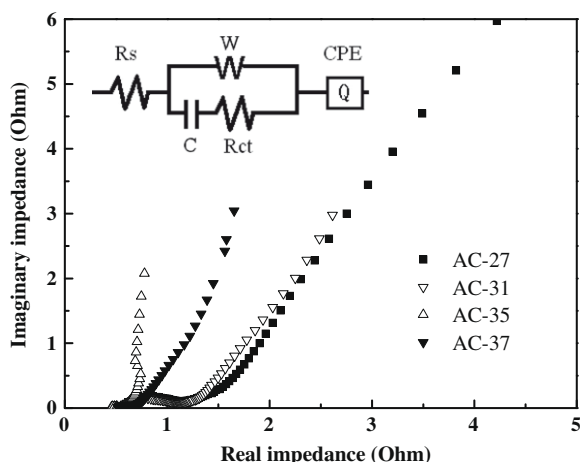


Fig. 9 – EIS and equivalent circuit model of AC electrodes.

macropores in ACs are helpful for the fast transportation of ions during the charge–discharge process.

The variation of the energy density of AC-35 capacitor with the cycle number is shown in Fig. 8(b). For comparison, AC-35 was heated at 800 °C for 1 h under vacuum with an aim of understanding the effect of heat treatment on the EDLC energy density and stability. Fig. 8(b) shows that the energy density of AC-35 capacitor drops from 11.6 to 9.3 Wh/kg after 100 cycles with an energy retention ratio of 80.2%, then further decreases but slowly, and remains at 8.0 Wh/kg after 800 cycles with an energy retention ratio of 68.8%. For the capacitor

made of AC-35 heated at 800 °C, the energy density drops from 5.0 to 3.9 Wh/kg after 800 cycles with an energy retention ratio of 78.0% that is about 10% higher than the untreated AC-35. This implies that the heat treatment can help improve the stability of AC capacitor to some degree but with some loss in energy density.

3.3.3. EIS of AC electrode

The impedance spectra of different AC electrodes are shown in Fig. 9, in which the inset is the equivalent circuit model of AC electrodes that is used to explain the characteristics of EIS. The equivalent circuit model reveals that the whole capacitor circuit is constituted by R_s , W , R_{ct} , C and Q , here R_s is the sum of the contact resistance and material resistance (electrode materials, electrolyte and separator); W is the Warburg resistance when the matter moves in solution, exhibiting a line when the slope is 1; R_{ct} is the resistance for blocking ions from entering the pores of electrode materials, and for blocking the movement of ions in solution and separator; C and Q are capacitor layer formed in the charge–discharge process. It can be seen that in comparison with other AC electrodes, the AC-35 electrode has smaller value that crosses with the real axis at 0.47 Ω , indicating that AC-35 electrode has lower contact resistance and better conductivity than other three electrodes. At lower frequency range, the curve for AC-35 is nearly vertical to the real axis, while for AC-27 and AC-31, a large slope in the curve can be seen, implies that it is difficult for the ions in electrolyte to enter the pores of AC-27 and AC-31. In other words, the porous

Table 3 – Parameters of the equivalent circuit for different AC electrodes.

Electrode sample	R_s (Ω/cm^2)	R_{ct} (Ω/cm^2)	$W(Y)$ ($\text{S}/\text{s}^{0.5}/\text{cm}^2$)	C (F/cm^2)	$Q(Y)$ ($\text{S}/\text{s}^n/\text{cm}^2$)	n	χ^2
AC-27	0.4780	0.7750	0.0156	4.33	1.038	0.55	1.27e-03
AC-31	0.4726	0.7198	0.0179	11.06	1.898	0.57	1.06e-03
AC-35	0.0550	0.3446	3.98E-19	6.52	3.538	0.13	1.25e-03
AC-37	0.4753	0.1959	0.0484	7.59	2.436	0.57	4.35e-04

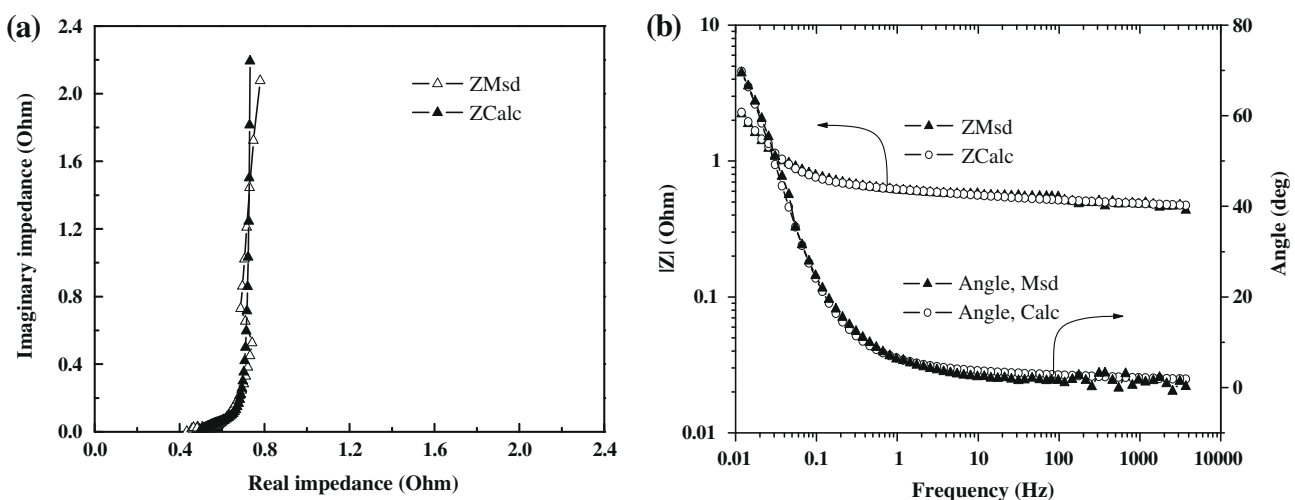


Fig. 10 – (a) Nyquist plot of AC-35 electrodes; (b) Bode plot of AC-35 electrodes.

structure of AC-35 provides a better channel for the movement of the ions.

The impedance data of different AC electrodes simulated using ZSimpWin software are shown in Table 3. Double layer capacitance is expressed as constant phase angle element (Q), and n is the correction factor between 0 and 1. The square error (χ^2) for different impedance spectra of AC electrodes is relatively small, ranging from 4.35×10^{-4} to 1.25×10^{-3} , evidencing that the equivalent circuit model adopted is correct in the present study. Table 3 also shows that the contact resistance (R_s) for AC-35 is the smallest among the tested AC electrodes, indicating the conductivity of AC-35 is the best. For the AC-35 electrode, the W and R_{ct} are also smaller than that of AC-27 and AC-31, implying that the ion transport resistance in the case of AC-35 is smaller.

Fig. 10(a) is Nyquist plot and Fig. 10(b) is the Bode plot of AC-35 electrodes, in which both the measured (Msd.) and calculated (Calc.) EIS data using ZSimpWin software according to the equivalent circuit model in Fig. 9 are shown. It can be clearly seen from Fig. 10(a) that the measured and calculated EIS data for AC-35 electrode are in good agreement. Fig. 10(b) shows that the phase angle is 70° (the ideal one should be 90°) at lower frequency limitation, further evidencing the good capacitive property of AC-35 electrodes.

4. Conclusions

High performance ACs for EDLCs are prepared by microwave-assisted activation of petroleum coke with KOH as activating agent. The influence of activation time on AC properties has been addressed in terms of the pore structure and electrochemical properties of the ACs. It has been found that the S_{BET} and the V_t of ACs goes through a maximum as the activation time increases, of which the S_{BET} is $2312 \text{ m}^2/\text{g}$ for AC-35 made in 35 min of activation time. The specific capacitance of AC-35 electrode at a current density of 50 mA/g is 342.8 F/g , and remains at 245.6 F/g even after 800 cycles with an energy density of the capacitor being at 8.0 Wh/kg . The results demonstrate that microwave-assisted activation technique is of potential to make ACs with high performance in EDLCs because of its high efficiency, less time and low energy consumption.

Acknowledgements

This work is partly supported by the NSFC (Nos. 50802002, 20836002 and 20725619), Natural Science Foundation of Anhui Province (KJ2008A120 and 2008JQ1026ZD), and Foundation of Provincial Innovative Group for Processing and Clean Utilization of Coal Resource.

REFERENCES

- [1] Huang JS, Sumpter BG, Meunier V. A universal model for nanoporous carbon supercapacitors applicable to diverse pore regimes, carbon materials, and electrolytes. *Chem Eur J* 2008;14:6614–26.
- [2] Endo M, Kim YJ, Ohta H, Ishii K, Inoue T, Hayashi T, et al. Morphology and organic EDLC applications of chemically activated AR-resin-based carbons. *Carbon* 2002;40:2613–26.
- [3] Wang DW, Li F, Liu M, Lu GQ, Cheng HM. 3D aperiodic hierarchical porous graphitic carbon material for high-rate electrochemical capacitive energy storage. *Angew Chem Int Ed* 2008;47:373–6.
- [4] Lota G, Frackowiak E. Striking capacitance of carbon/iodide interface. *Electrochem Commun* 2009;11:87–90.
- [5] Wang CC, Hu CC. Electrochemical catalytic modification of activated carbon fabrics by ruthenium chloride for supercapacitors. *Carbon* 2005;43:1926–35.
- [6] Nam KW, Lee CW, Yang XQ, Cho BW, Yoon WS, Kim KB. Electrodeposited manganese oxides on three-dimensional carbon nanotube substrate: supercapacitive behaviour in aqueous and organic electrolytes. *J Power Sources* 2009;188:323–31.
- [7] Yagmur E, Ozmak M, Aktas Z. A novel method for production of activated carbon from waste tea by chemical activation with microwave energy. *Fuel* 2008;87:3278–85.
- [8] Valente NJM, Carrott PJM, Ribeiro CML, Menéndez JA. Preparation and modification of activated carbon fibres by microwave heating. *Carbon* 2004;42:1315–20.
- [9] Ji YB, Li TH, Zhu L, Wang XX, Lin QL. Preparation of activated carbons by microwave heating KOH activation. *Appl Surf Sci* 2007;254:506–12.
- [10] Ania CO, Parra JB, Menéndez JA, Pis JJ. Effect of microwave and conventional regeneration on the microporous and mesoporous network and on the adsorptive capacity of activated carbons. *Micropor Mesopor Mater* 2005;85:7–15.
- [11] Li W, Zhang LB, Peng JH, Li N, Zhu XY. Preparation of high surface area activated carbons from tobacco stems with K_2CO_3 activation using microwave radiation. *Ind Crops Prod* 2008;27:341–7.
- [12] Xu B, Wu F, Chen RJ, Cao GP, Chen S, Zhou ZM, et al. Highly mesoporous and high surface area carbon: a high capacitance electrode material for EDLCs with various electrolytes. *Electrochem Commun* 2008;10:795–7.
- [13] Olivares-Marín M, Fernández-González C, Macías-García A, Gómez-Serrano V. Preparation of activated carbons from cherry stones by activation with potassium hydroxide. *Appl Surf Sci* 2006;252:5980–3.
- [14] Elizalde-González MP, Hernández-Montoya V. Characterization of mango pit as raw material in the preparation of activated carbon for wastewater treatment. *Biochem Eng J* 2007;36:230–8.
- [15] Baccar R, Bouzid J, Feki M, Montiel A. Preparation of activated carbon from Tunisian olive-waste cakes and its application for adsorption of heavy metal ions. *J Hazard Mater* 2009;162:1522–9.
- [16] Zhu HM, Yan JH, Jiang XG, Lai YE, Cen KF. Study on pyrolysis of typical medical waste materials by using TG-FTIR analysis. *J Hazard Mater* 2008;153:670–6.
- [17] He XJ, Lei JW, Geng YJ, Zhang XY, Wu MB, Zheng MD. Preparation of microporous activated carbon and its electrochemical performance for electric double layer capacitor. *J Phys Chem Solids* 2009;70:738–44.
- [18] Lillo-Ródenas MA, Cazorla-Amorós D, Linares-Solano A. Understanding chemical reactions between carbons and NaOH and KOH – an insight into the chemical activation mechanism. *Carbon* 2003;41:267–75.
- [19] Zhang CX, Long DH, Xing BL, Qiao WM, Zhang R, Zhan L, et al. The superior electrochemical performance of oxygen-rich activated carbons prepared from bituminous coal. *Electrochem Commun* 2008;10:1809–11.
- [20] Portet C, Yushin G, Gogotsi Y. Effect of carbon particle size on electrochemical performance of EDLC. *J Electrochem Soc* 2008;155:A531–6.

- [21] Hu CC, Wang CC. Effects of electrolytes and electrochemical pretreatments on the capacitive characteristics of activated carbon fabrics for supercapacitors. *J Power Sources* 2004;125:299–308.
- [22] Qu D, Shi H. Studies of activated carbons used in double-layer capacitors. *J Power Sources* 1998;74:99–107.
- [23] Frackowiak E, Béguin F. Carbon materials for the electrochemical storage of energy in capacitors. *Carbon* 2001;39:937–50.
- [24] Lozano-Castelló D, Cazorla-Amorós D, Linares-Solano A, Shiraishi S, Kurihara H, Oya A. Influence of pore structure and surface chemistry on electric double layer capacitance in non-aqueous electrolyte. *Carbon* 2003;41:1765–75.
- [25] He XJ, Jiang L, Yan SC, Lei JW, Zheng MD, Shui HF. Direct synthesis of porous carbon nanotubes and its performance as conducting material of supercapacitor electrode. *Diamond Relat Mater* 2008;17:993–8.
- [26] Varma S, Rempe SB. Coordination numbers of alkali metal ions in aqueous solutions. *Biophys Chem* 2006;124:192–9.
- [27] Zhu M, Weber CJ, Yang Y, Konuma M, Starke U, Kern K, et al. Chemical and electrochemical ageing of carbon materials used in supercapacitor electrodes. *Carbon* 2008;46:1829–40.
- [28] Fang B, Wei YZ, Kumagai M. Modified carbon materials for high-rate EDLCs application. *J Power Sources* 2006;155:487–91.
- [29] Prabakaran SRS, Vimala R, Zainal Z. Nanostructured mesoporous carbon as electrodes for supercapacitors. *J Power Sources* 2006;161:730–6.
- [30] Chmiola J, Yushin G, Gogotsi Y, Portet C, Simon P, Taberna PL. Anomalous increase in carbon capacitance at pore sizes less than 1 nanometer. *Science* 2006;313:1760–3.